

# Characterization of Various shaped 5 GHz TFBARs Based on 3D Full-wave Modeling

Yong-Dae Kim<sup>1</sup>, Kook-Hyun Sunwoo<sup>2</sup>, Sung-Hoon Choa<sup>2</sup>, Duck-Hwan Kim<sup>2</sup>,  
In-Sang Song<sup>2</sup>, Jong-Gwan Yook<sup>1</sup>

<sup>1</sup>Dept. of Electrical and Electronic Eng., Yonsei Univ., 134 Shinchon-dong, Seodaemun-gu, Seoul 120-749, Korea

<sup>2</sup>MEMS Lab, Samsung Advanced Institute of Technology,  
Mt, 14-1, Nongseo-Ri, Giheung-Eup, Gyeonggi-Do, 449-712, Korea

**Abstract** — In this paper, three dimensional finite element method is used for the analysis of thin film bulk acoustic wave resonator (TFBAR) at 5GHz. The TFBAR is placed on thin membrane after removal of substrate material for the suppression of loading effects and three different geometries (rectangular, polygonal and circular) are implemented and modeled. The size of fabricated TFBAR are from 100x100  $\mu\text{m}^2$  to 200x200  $\mu\text{m}^2$  and full-wave modeled results are compared with the measurement. It is found that the modeled and measured results agree within 1% in terms of series and parallel resonant frequencies. Furthermore, the different shapes of TFBAR revealed slightly different bandwidth characteristics, which is defined on frequency spacing between the series and parallel resonant frequencies. The another goal of this work is to study the variation of the size of resonator on how affects the performance of TFBAR. As the size of resonator increase, the electrical impedance of TFBAR decrease at the resonant frequencies and out of resonant frequencies. These phenomena contribute to improve the effects of the attenuations of TFBAR filter in stop-band to some degree.

## I. INTRODUCTION

Recently, various types of mobile communication systems are under development to provide high data rate communication services. In practice, high frequency around 5 GHz band has been actively employed as Wireless Local Area Network (WLAN) application. In these systems, the role of RF front-end-module is very important and RF band pass filter plays crucial roles in miniaturization of RF systems. One strong candidate of RF band pass filter is a TFBAR filter which uses piezoelectric resonator. 5 GHz WLAN applications require 200 MHz bandwidth at center frequency of 5250 MHz. to achieve bandwidth of 200 MHz using the TFBAR, frequency spacing between series and parallel resonant frequencies, should be at least more than 100 MHz.

For accurate and effective modeling of piezoelectric and electromechanical characteristics of TFBAR, various approaches have been introduced in the literature [1]-[3]. Among those, Mason model has been most widely used to analyze and simulate the 1-D vertical structure of TFBAR. However, for the accurate and reliable TFBAR filter design, it is necessary to model three dimensional geometry of unit resonator cell in detail and finite element method (FEM) is an appropriate candidate for three dimensional analysis of TFBAR. Because FEM is a

strictly numerical technique, it could provide insights into the underlying physics and phenomena. In addition, it is possible to accommodate arbitrary geometrical parameters, material constants, as well as piezoelectricity with reasonable accuracy and modeling speed. Thin-film BAW technology opens a door to miniaturize on wafer resonators and filters with GHz-ranges operating frequencies, which is compatible with active RF circuits [4]-[5]. The simulated and fabricated thin film BAW resonators in this paper bears membrane-type resonator configuration. The top and bottom electrode materials are molybdenum (Mo) and aluminum nitride (AlN) is used for piezoelectric material. while the membrane is made of thin AlN.

Furthermore, in this work, the impedance characteristics of TFBAR are investigated and described on the variation of TFBAR size and it is found that the impedance characteristics of TFBAR are directly related to the size of resonator. The configurations of TFBAR are structurally extended and realized for considering the impedance tendency of TFBAR based on 3D full-wave modeling.

## II. FEM MODELING AND FABRICATION OF TFBAR

The practical structure to simulate a TFBAR is equal to as shown in Fig. 1. For piezoelectric and membrane material, aluminum nitride (AlN) is selected in this modeling, while molybdenum (Mo) is employed for the top and bottom electrodes. In applying RF signal to the TFBAR, the propagation range of acoustic wave in the TFBAR is confined between the top and bottom electrodes loaded with AlN membrane

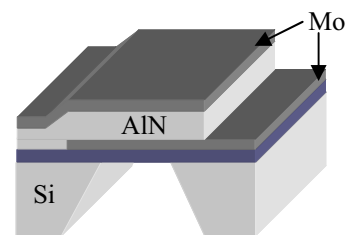


Figure 1 Vertical structure of membrane-type TFBAR

Fig.2 indicates three dimensional finite element model of TFBAR. It is considered that a volume constitutes the problem domain as illustrated in Fig.2 for BAW resonator.

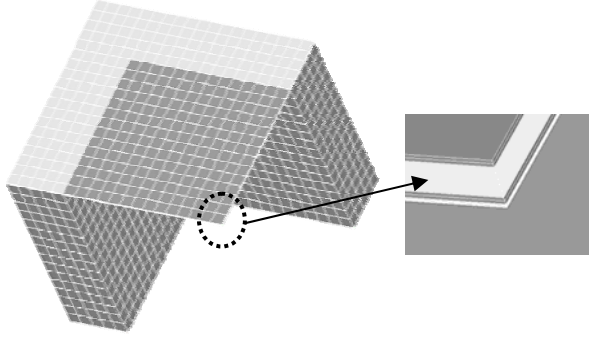


Figure 2 A quarter of finite element model in TFBAR

Table 1 Mechanical properties of material

Material properties	Young's modulus GPa	Poisson ratio $\sigma$	Density Kg/m <sup>3</sup>
AlN	-	-	3260
Mo	350	0.32	11020

In finite element method, the physical problem domain is discretized, that is, subdivided into small elementary volumes called elements. In the same way, the polygonal and circular resonators are modeled as well as the rectangular resonator. After the fabrication of TFBAR, fig.3 shows the top-view and the cross-sectional TEM photograph of fabricated TFBAR.

Piezoelectric materials such as AlN and ZnO are anisotropic materials. The characteristics of these piezoelectric materials have the link between electrical and mechanical phenomena and vice versa. The governing constitutive equations for piezoelectricity are as follows [6]:

$$\begin{cases} \{T\} = [c]\{S\} - [e]\{E\} \\ \{D\} = [e]^T\{S\} + [\epsilon]\{E\} \end{cases} \quad (1)$$

When applied to a three-dimensional geometry, the above equations take a relatively complicated form because the elastic stiffness components  $[c]$  couple two  $3 \times 3$  matrices. In here, the elastic stiffness constant  $[c]$  has a  $6 \times 6$  matrix form.

The most important factors to affect the resonant frequency of TFBAR as well as thickness of material are material density and elastic stiffness constants. However, the material parameters given in the references are not absolutely accurate. Moreover, the mechanical properties are dependent on the fabrication process. Therefore, the mechanical parameters are

optimized from the previous measured data of the fabricated TFBAR. Mechanical properties of materials are summarized in Table 1. As mentioned from the above, because of AlN being anisotropic material, Young's modulus and Poisson's ratio of AlN are determined by the elastic stiffness constants.

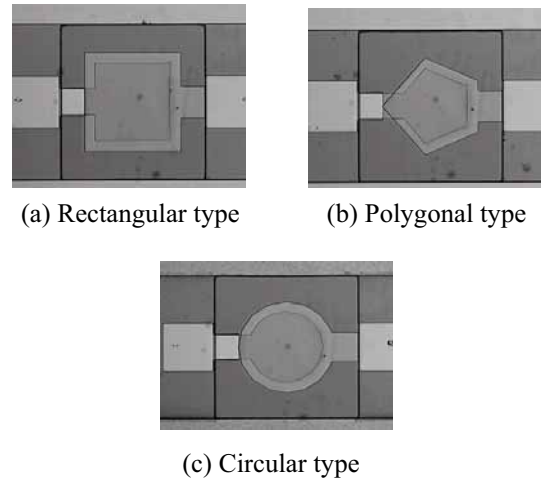


Figure 3 Top-view of fabricated various shaped FBARs

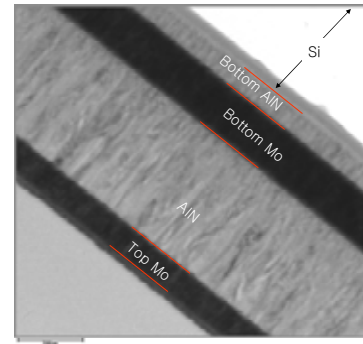
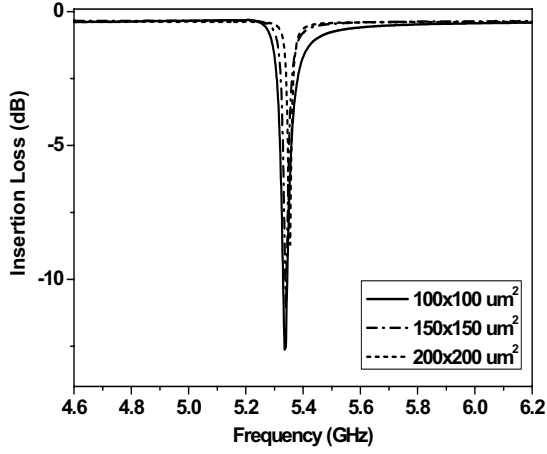


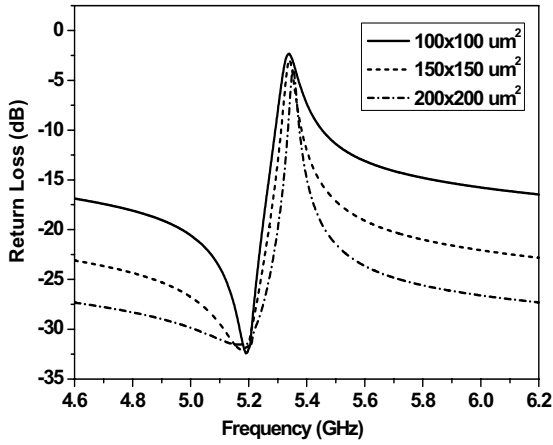
Figure 4 Cross-sectional TEM photograph of FBAR

### III. RESULTS AND DISCUSSION

To validate the effectiveness and performance of FEM simulation, membrane-type TFBAR is fabricated as shown in Figure 3 and 4. The fabricated shapes of TFBAR are polygonal, rectangular and circular. The area sizes of TFBAR are  $100 \times 100 \text{ um}^2$ ,  $150 \times 150 \text{ um}^2$  and  $200 \times 200 \text{ um}^2$ . In Figure 5, the series and parallel resonant frequencies of fabricated TFBAR are 5.191 GHz and 5.335 GHz. In simulation results, the series and parallel resonant frequency are 5.207 GHz and 5.35 GHz and the bandwidth of measurement and simulation are 144 MHz and 143 MHz. In result, the difference of resonant frequency turned out to be about 16 MHz. The error range in resonant frequency showed small difference with measurements, including the circular and rectangular shapes of TFBAR. It was also observed that the insertion loss of resonator in series resonant frequency is -0.31dB. However, as shown in Figure 6, the amplitude of electrical impedance has not good agreements with the measurement near the resonant frequencies. The characteristics of resonance became appeared to be good in the simulation rather than in the measurement. The discrepancy of the amplitudes of electrical impedances between the measured and simulated resonant frequency could be caused from various reasons. Acoustic wave propagation losses (attenuation) are caused by various physical mechanisms.



(a) Insertion loss tendency of fabricated FBAR



(b) Return loss tendency of fabricated FBAR

Figure 5 Losses characteristics due to the variation of FBAR sizes

For instance, in material with finite-size grains, scattering losses are existed and thickness error could be caused by roughness problems. Moreover the elastic stiffness properties used in the simulation are not absolute and dependent on the fabrication process. Various imperfections in materials, such as dislocations in a crystal lattice will also cause scattering losses. However, FEM-based simulation was not perfectly considered these physical material characteristics and acoustic losses into the TFBAR design.

As indicated in Figure 5, Losses characteristics of all fabricated TFBARs exhibit with respect to various sizes of TFBAR. As the size of TFBAR increases, the return losses as well as insertion losses of TFBARs exhibit different loss characteristics while remaining nearly the resonant frequencies. There are little variations of 5 to 20 MHz in resonant frequencies because as the size of TFBAR become larger, the electrical and mechanical capacitances increase, but the mechanical inductance decreases.

However, though the characteristics of resonance are usually affected by the material thickness, the AlN-film

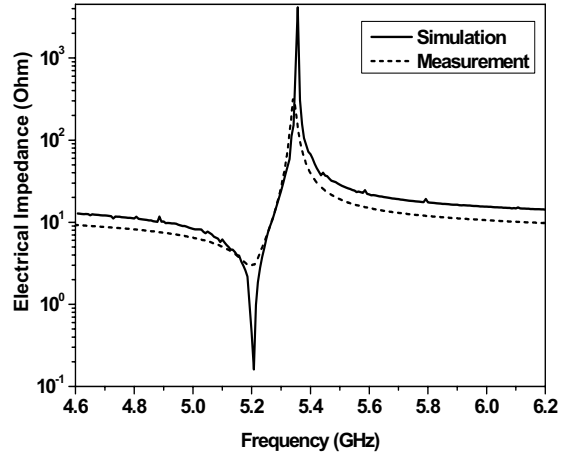


Figure 6 Compared impedance characteristics of FEM simulation and measurement

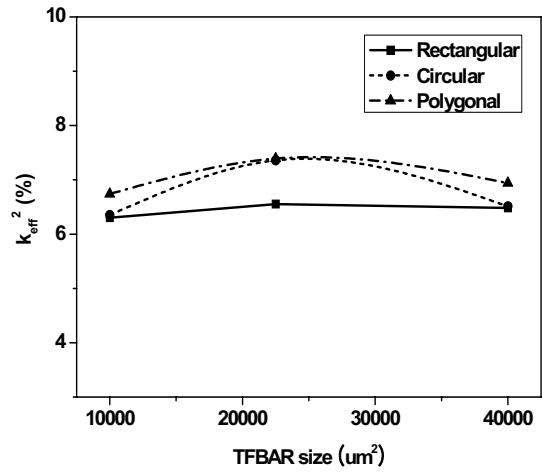


Figure 7 Characteristics of Effective electro-magnetic coupling factor as function of TFBAR size

texture also impacts on the resonance characteristics of TFBAR. The electromechanical coupling is directly related to the degree of c-axis orientation of the AlN film for FBARs utilizing the thickness excited (TE) longitudinal mode. The effective coupling coefficient constants ( $k_{eff}^2$ ) are calculated from the series resonant frequency  $f_s$  and parallel resonant frequency  $f_p$  as follows [6]:

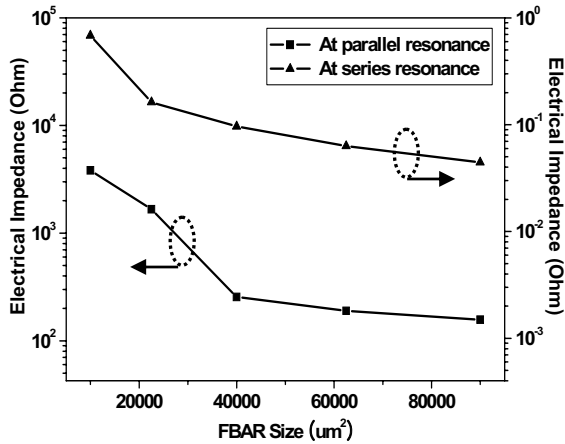
$$k_{eff}^2 = \frac{\left( \frac{\pi f_s}{2 f_p} \right)}{\tan \left( \frac{\pi f_s}{2 f_p} \right)} \quad (2)$$

As clearly shown in Figure 7, all of fabricated TFBAR reveal that show different values of  $k_{eff}^2$  in despite of same material thickness of TFBAR. Although fabricated TFBARs have the identical fabrication conditions except for the various size and shape of TFBAR, Figure 7 means that some degrees of c-axis-directed AlN film quality in piezoelectric material have effects on the frequency characteristics of TFBAR. Moreover, in application of TFBAR filter, the characteristics of  $k_{eff}^2$  affect dominantly the bandwidth of TFBAR filter. Fabricated

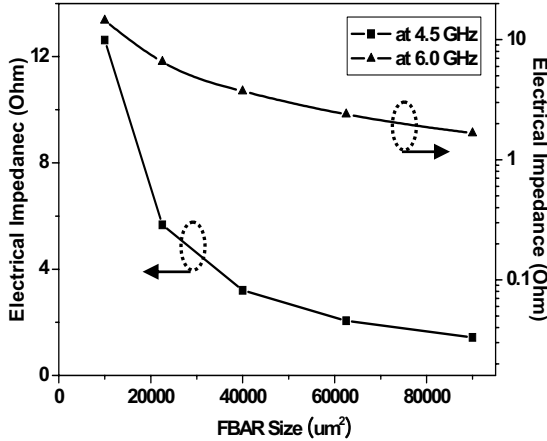
TFBARs revealed the  $k_{\text{eff}}^2$  of average 6.5% and the bandwidth of more than 140 MHz.

#### IV. CHARACTERIZATION OF ELECTRICAL IMPEDANCE

It was previously reported that the loss characteristics of TFBAR were affected due to the variations of TFBAR size. For the development of analyzing the loss characteristics of TFBAR, the characterization of electrical impedance is represented based on the 3-D full-wave modeling as well as circuit modeling [7].



(a) Electrical impedance tendency at resonant frequencies



(b) Electrical impedance out of resonant frequencies

Figure 8 Characteristics of electrical impedance due to the various sizes of TFBAR

The characteristics of electrical impedance tendency in Figure 8 describe that as the size of TFBAR increases gradually, the magnitude of electrical impedance decreases. In application of filter used TFBAR as resonator, the constitution of optimal TFBAR size ratio which means the ratio of shunt resonator to series resonator and vice versa characterizes the performance of filter. However, although if the size of TFBAR becomes increased, the attenuation characteristics of TFBAR filter

could be improved to some degrees, there are limitations of increasing TFBAR size for impedance-mismatching problems.

At higher frequency such as above 5 GHz, in results of filter simulation and experimental test, it revealed that the unit TFBAR sizes used in 5 GHz band-pass filter require small dimensions for reasonable impedance-matching effects. It is expected that as frequency become higher, the size of TFBAR and associated filter decrease and begin to affect the requirement of packaging and filter performance.

#### V. CONCLUSION

We indicated that 3D FEM-based full-wave modeling is developed and applied for various shape of 5 GHz TFBAR geometry. Fabricated have the  $k_{\text{eff}}^2$  of 6.5% and the bandwidth of more than 140 MHz. It is investigated and analyzed on the characteristics of electrical impedance due to the various TFBAR sizes. In high frequency such as 5 GHz or above, the size of TFBAR and associated filter should be small dimensions for reasonable impedance-matching effects though the simulation and experimental tests. At present, more considerations are required for increasing  $k_{\text{eff}}^2$  of TFBAR. In addition, the change of thickness is very sensitive in 5 GHz-band. The thickness control of material remain as technical challenges because very small amount of over or under deposition could cause shifts in resonant frequency

#### ACKNOWLEDGEMENT

The authors wish to acknowledge Samsung Advanced Institute of Technology for fabricating TFBAR and advising the technical supports.

#### REFERENCES

- [1] J.D. Larson III, P.D. Bradley, S. Wartenberg and R.C. Ruby, "Modified Butterworth-Van Dyke circuit for FBAR resonators and automated measurement system," *2000 IEEE Ultrasonics and Symposium Digest*, vol. 1, pp. 863-868, 2000
- [2] K. M. Lakin, "Modeling of Thin Film Resonators and Filters," *1992 IEEE MTT-S Digest*, vol.1, pp 149-152, 1992
- [3] S. A. Morris and C. G. Hutchens, "Implementation of Mason's Model on Circuit Analysis Program," *IEEE Trans. On UFFC*, vol. 33, No. 3, pp295-298, May 1986
- [4] H. Satoh, H. Suzuki, C. Takahashi, C. Narahara, and Y. Ebata "A 400 MHz one-chip oscillator using an air-gap type thin film resonator," in *Proc. IEEE Ultrason. Symp.*, pp. 363-368, 1987.
- [5] W. A. Burkland, A. R. Landin, G. R. Kline, and R. S. Ketcham, "A thin-film bulk-acoustic wave resonator controlled oscillator on silicon," *IEEE Electron. Device Lett.*, vol. EDL-8, no. 11, pp. 531-533, 1987.
- [6] J. Rosenbaum, *Bulk Acoustic Wave Theory and Devices*, Artech House, Norwood, 1988
- [7] J. S. Kim, Y. D. Kim, M. G. Gu, J. G. Yook, "New Modeling of TFBAR and On-wafer Inductor Effects on the TFBAR Ladder Filter Performance," *2004 IEEE MTT-S*, vol. 1, pp.379-382